Collateral flows in patients with aortic coarctation: a clinical and biomechanical study

Amandine Martin, Herve Corbineau, Jean Philippe Verhoye, Mathieu Lederlin, Agnès Drochon

Collateral flows in patients with aortic coarctation: a clinical and biomechanical study

Amandine Martin[1], Hervé Corbineau[1], Jean-Philippe Verhoye[1], Mathieu Lederlin[2] and Agnes Drochon[*3],

[1]*Chirurgie Thoracique et Cardiovasculaire, CHU Pontchaillou, 2, rue Henri Le Guilloux,*
35033 Rennes cedex   France
[2]*Département d'Imagerie Coeur-Vaisseaux, CHU Pontchaillou, 2, rue Henri Le Guilloux,*
35033 Rennes cedex   France
[3]*Université de Technologie de Compiègne and Sorbonne Université, UMR 7338, GB, Royallieu,*
BP 20529, 60205 Compiègne   France

Abstract. Coarctation of aorta is a congenital anomaly characterized by a narrowing segment between the aortic arch and the descending aorta. This stenosis is responsible for upper body hypertension and the recruitment of a collateral network via the intercostal arteries to improve lower body perfusion. However, hemodynamic perturbations along the aorta have not been completely studied.

The objective of this work is to analyze the collateral network of patients with aortic coarctation who required surgical repair. MRI was performed to obtain hemodynamic parameters such as the variation of flow along the descending thoracic aorta and an estimation of the collateral flow. The shape of the aorta was also studied. Both morphological elements and hemodynamic parameters of aortic coarctation may be quite useful to determine consequences of aortic narrowing and the best moment to propose surgical repair or imaging monitoring. We also expect giving more information on the collateral network to develop modelisation of this element.

Introduction

∗Corresponding author, PhD, E-mail: agnes.drochon@utc.fr
[a] MD, E-mail: amandine.martin@chu-rennes.fr
[b] MD, Pr , E-mail: herve.corbineau@chu-rennes.fr
[c] MD, Pr , E-mail: jean-philippe.verhoye@chu-rennes.fr
[d] MD, Pr , E-mail: mathieu.lederlin@chu-rennes.fr

Coarctation of aorta is a congenital aortic anomaly characterized by a narrowing segment of the aorta just behind the left subclavian artery origin. This stenosis induces a higher arterial pressure before the constriction and is responsible for a higher morbidity and mortality due to upper body hypertension, left ventricular dysfunction, cerebral and aortic aneurysms and premature coronary artery disease.… [1, 2].

As a result, coarctation of aorta has been found to impact the blood distribution in the arteries leaving the aortic arch. In a standard situation, the proportion of blood ejected by the heart is 15% in the brachiocephalic artery, 7.5% in both left common carotid artery and the left subclavian artery and 70% in the descending aorta. Wittberg *et al.* [3] have found a decreased proportion of blood flow into the descending aorta in patients with aortic coarctation, while the proportion of blood flow in each supra-aortic vessels have increased in comparison to a normal thoracic aorta. Moreover, this redistribution of blood affects the wall shear stresses that can reach up to 10 Pa in some cases into the constriction against 3 Pa in a normal aorta.

According to the severity of the coarctation, a variable collateral network may develop to provide blood flow to the lower body via the subclavian, the internal thoracic and the intercostal arteries. Indeed, intercostal arteries receive between 7% and 11% of the flow from the descending aorta in a standard situation, whereas a reverse flow undergoes from the internal thoracic to the descending aorta for patients with aortic coarctation to compensate hypoperfusion of the lower body [4].

The severity of aortic coarctation is assessed by the pressure gradient (ΔP) along the stenosis, which is evaluated by an echocardiography or invasive cardiac catheterization. A value of (ΔP) greater than 20 mmHg is an indication to treat this pathology [5, 6]. However, ultrasound examinations are less efficient in old children and adults and, moreover, some authors think that a large amount of collateral flow entering the descending aorta raises pressure beyond the coarctation and may minimize the estimation of the severity of the coarctation [1, 5]. Nowadays, magnetic resonance imaging (MRI) is able to provide both hemodynamic and anatomic parameters of the aorta and has been recommended to follow patients with native or operated aortic coarctation from 2010 [2, 7, 8].

Our objective is to explore the collateral network in patients with native or repaired coarctation of aorta by MRI before and after corrective surgery. Collateral flow is estimated by the variation of flow along the descending thoracic aorta. In association with morphologic data, these informations might help physicians to evaluate consequences of aortic coarctation, to make decision for repair, and to monitor the patient outcome after corrective surgery. This is important, indeed, because, in some patients, some problems remain after surgery. For example, arterial hypertension often persists after correction [9-10].

Materials and methods

Four adult patients underwent a surgical correction of aortic coarctation in the Thoracic and Cardiovascular Surgical Department at University Hospital of Rennes (France) and had given informed consent or assent for this study. Patients' characteristics are summarized in Table 1. All patients had a late diagnosis of native aortic coarctation complicated by arterial hypertension and underwent different surgical repairs. One patient (Patient 3) presented symptoms of low body hypoperfusion (intermittent claudication). Associated lesion was an ascending aorta aneurysm without indication of treatment (Patient 1) and aortic arch hypoplasia (Patient 2), which was corrected simultaneously.

According to Ou *et al.* [11], three types of aortic arch shape were defined with the ratio of the arch height (h) over its width (l). An elevated h/l ratio (0.83 ± 0.14) was associated to a gothic (angulated) shape of the arch. The value we obtain for Patient 1 (h/l = 0.81) falls exactly in this range. A crenel arch is characterized by a double angulation of the thoracic aorta between ascending and cross of the aorta and between the cross and the descending aorta, whereas a normal arch has an harmonious curvature. As it has been nicely demonstrated by Hope et al. [2], the geometry of the arch has a major influence on the flow patterns.

The pressure gradient, ΔP, across the coarctation was estimated by Doppler echocardiography.

Every patient had a postoperative cardiac-gated, 3D, phase-contrast (PC) MRI and one patient (Patient 4) had a pre-operative examination. Five data collection points (Figure 1) were chosen along the aorta:
- S1 : ascending aorta
- S2 : distal aortic arch, just after left subclavian artery
- S3 : coarcted segment of the aorta (native or repaired)
- S4 : proximal segment of the descending aorta, after the coarcted zone
- S5 : distal segment of the descending aorta, at the diaphragm level

Time-dependent velocities (mean over the section), $V_i(t)$ (i = 1 to 5) were recorded for each aortic sections (S_i, i = 1 to 5), as well as the corresponding areas $A_i(t)$ (i = 1 to 5). Flow rates, $Q_i(t)$, i = 1 to 5, were obtained as: $Q_i(t) = V_i(t) \times A_i(t)$. Reynolds numbers, $Re_i(t)$ were calculated according to the classical definition in a cylindrical conduit $Re_i(t) = \rho V_i(t) D_i(t) / \mu$, where $D_i(t)$ is the diameter of the vessel in the section "i", ρ is the density of blood (1050 kg/m^3) and μ is its dynamic viscosity (3.5 mPa.s).
The blood flow into the supra-aortic vessels, $Q_{SAV}(t)$, was calculated as $Q_{SAV}(t) = Q_1(t) - Q_2(t)$. In much the same way, the collateral flow rate $Q_{col}(t)$, was estimated by $Q_{col}(t) = Q_5(t) - Q_4(t)$, and the upper-body flow rate, $Q_{up}(t)$, by $Q_{up}(t) = Q_{SAV}(t) - Q_{col}(t)$.
The relative maximal variation of the area during a cardiac cycle in each section S_i was calculated by the ratio $(A_i^{maxi} - A_i^{mini}) / A_i^{mini}$. This quantity provides an estimation of the distensibility of the vessel: the greater is this ratio, the more distensible is the vessel at the place considered.
Besides, the mean area over the cardiac cycle, A_i^{mean}, was evaluated in each S_i. These quantities were then used to estimate the severity of the constriction. We introduced two criterias:
i) the first one, called Sev1, was defined by Steffens *et al.* [1] as:
$$Sev1 = A_3^{mean} / \tfrac{1}{2} (A_2^{mean} + A_4^{mean})$$
Use of this index for postoperative analysis evaluated the efficiency of the surgical correction : the closer to 1 is the value, the better is the surgical repair.
ii) the second one, called Sev2, was defined by Goubergrits *et al.* [6] as :
$$Sev2 = (A_4^{mean} - A_3^{mean}) / A_4^{mean}$$
This index measured the relative decrease of area in S_3, as compared to the area in S_4: the closer to 1 is the value , the narrower is the aorta.
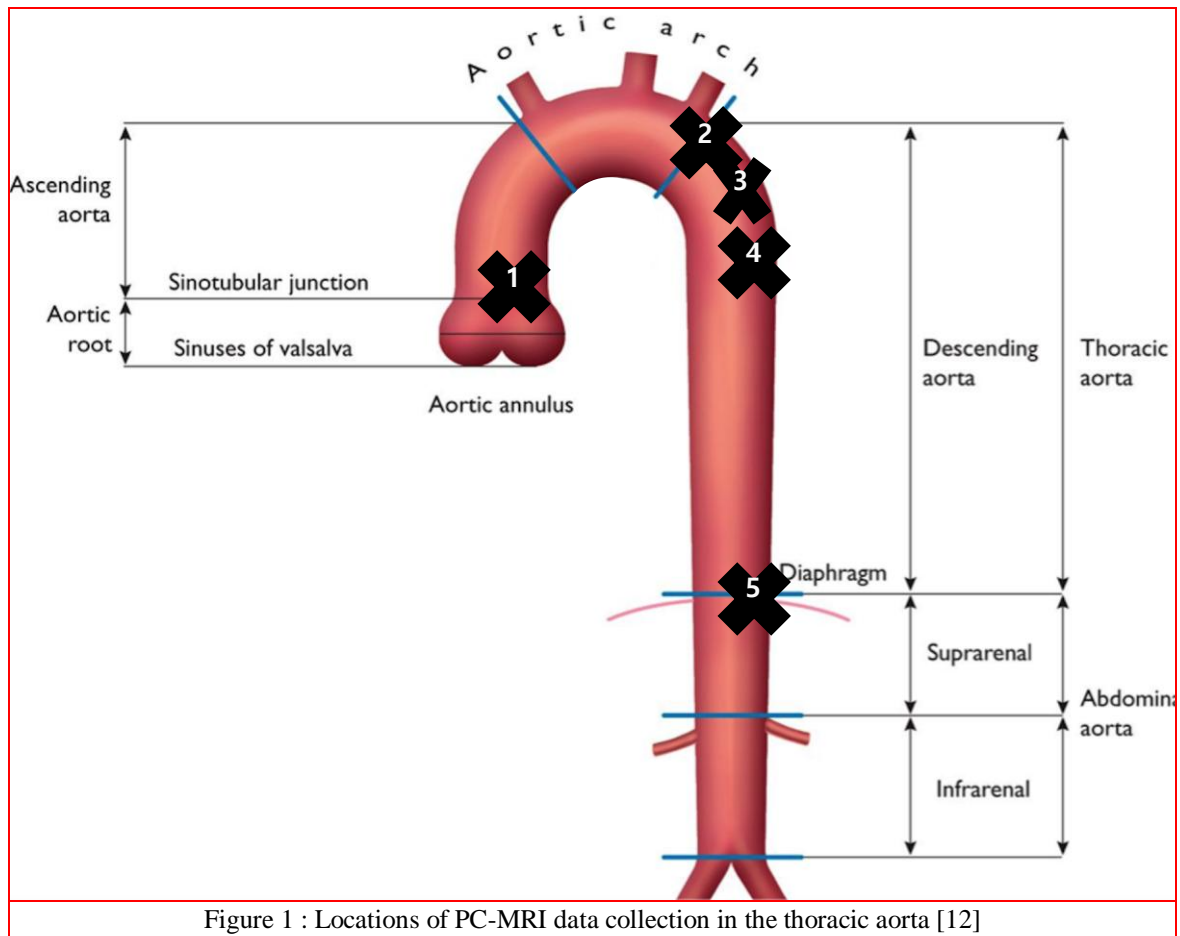
Figure 1 : Locations of PC-MRI data collection in the thoracic aorta [12]

Table 1 Patients' characteristics and clinical conditions. ΔP is the pressure gradient before surgery (mmHg)

Patients	Sex	Age (years)	ΔP	Type of Surgery	h / l (mm/mm)	Type of arch
Patient 1	M	31	65	Interposition tube graft	49.3/61	Gothic
Patient 2	F	45	40	Complete replacement of thoracic aorta	46.9/75.3	Normal
Patient 3	M	33	Not Avail.	Interposition tube graft	Not Avail.	Normal
Patient 4	F	60	40	Enlargement patch	32.6/73.2	Crenel

Results and discussion

Morphological data

Figure 2 represents preoperative areas $A_i(t)$ registered for Patient 4 and confirms the low area at the place of the constriction ($A_3(t)$). This may be seen also with the data of Table 2, and corresponds to an index Sev2 = 0.79, indicating a reduction of area of 79% in S_3, when compared to S_4. The index Sev1 was 0.17 and showed a reduction of area of 83% in S_3., when compared to the mean value of area in S_2 and S_4. Due to the fact that the coarcted segment of aorta (A_3) was very narrowed, the relative variation of area in S_3 was as large as the area itself and the ratio ($A^{max} – A^{min}$) / A^{min} equaled one. These preoperative data (areas and percent stenosis) fall exactly in the range of those given by Goubergrits *et al.* [6] in their Table2. In their experimental and theoretical models of aortic coarctation, Keshavarz-Motamed *et al.* [9] also consider a range of CoA severities from 50 to 90% reduction in area. The dilatation index is more difficult to compare to the literature, because it does not take into account the local pressure (not available in our study).

Post-operative areas $A_i(t)$ (mean values, maxi, mini) of the 4 patients are gathered in Table 3. These data allowed to calculate dilatation indexes presented in Table 4 and coarctation severities in Table 5.
There were some evident dispersion in these data due to the inter-patient variability (age, sex, cardiovascular risk factors, …) and to the different surgical procedures. The pre and postoperative analysis for Patient 4 showed clearly that surgery modified the mechanical response of the aorta wall to the pressure pulse, even if an obstruction (about 43% reduction in area) was still present after surgery (Table 5). The lowest distensibility was obtained at the constriction throat (in Section S_3) for Patient1 only. The lumen of the vessel in S_3 was totally restored for Patient 1 and 3 (Sev1 around 1); for Patient 2, the surgical correction gave an area A_3 after surgery of 86% of the mean of A_2 and A_4.
In the litterature, it has been demonstrated that patients with CoA have reduced proximal and distal aortic compliances. Thus, this factor could contribute to the persistant arterial hypertension even after a successful repair [9-11, 13]. In their computational simulation of aortic coarctation, LaDisa *et al.* [14] have adopted a value of 2.57 10^5 Pa for the Young modulus of normal aortas, 3.17 10^5 Pa in the case of a moderate native CoA, and 5.54 10^5 Pa in the case of a severe native CoA. However, O'Rourke and Cartmill [15] have explained that physical dimensions of the effectively pulsating part of the arterial system are considerably reduced in the coarctation of aorta. As a consequence, there are marked alterations in pulsatile hemodynamics in the proximal aorta and in upper body arteries. The coarctation of aorta, as well as the surgical repair, have obviously an impact on the pulse wave transmission, so that the interpretation of our measured quantity (A^{max}-A^{min})/A^{min} seems delicate …

Measured flow rates, velocities and associated Reynolds

    Pre-operative data (Patient 4)
Time-dependent flow rates $Q_i(t)$ are shown in Figure 3 and velocities $V_i(t)$ in Figure 4. The corresponding mean values of the flow rates, peak systolic velocities and peak systolic Reynolds are given in Tables 6, 7 and 8, respectively. As expected, during most of the systole, the flow rate

Q_1 was much higher than Q_2. From about mid-systole, Q_5 became higher than Q_4, which indicated that some collateral flow existed. Such an effect has been previously illustrated in the literature: see, for example, the Figure 3 in [1], the Figure 3 in [7], and the Figure 7 in [16]. These results are also quite similar to those presented in the Figure 4 of Hope *et al.* [2]. These authors present the case of a Patient with severe coarctation and collateral flow: the range of the ordinates is 2000ml/min to 14000 ml/min (or equivalently 33.33 ml/s to 233.33 ml/s); their "AsAo" flow rate is our Q_1, their "ProxDsAo" is our Q_4, their "Diaphragm" is our Q_5. As in our results, their curves for the proximal descending aorta and for the distal descending aorta are much more flat than the curve for the ascending aorta. However, in our Figure 3, one can notice that the flow rate Q_3 is lower than Q_4 and Q_5. This could be explained by some collateral flow arriving just after the coarctation.
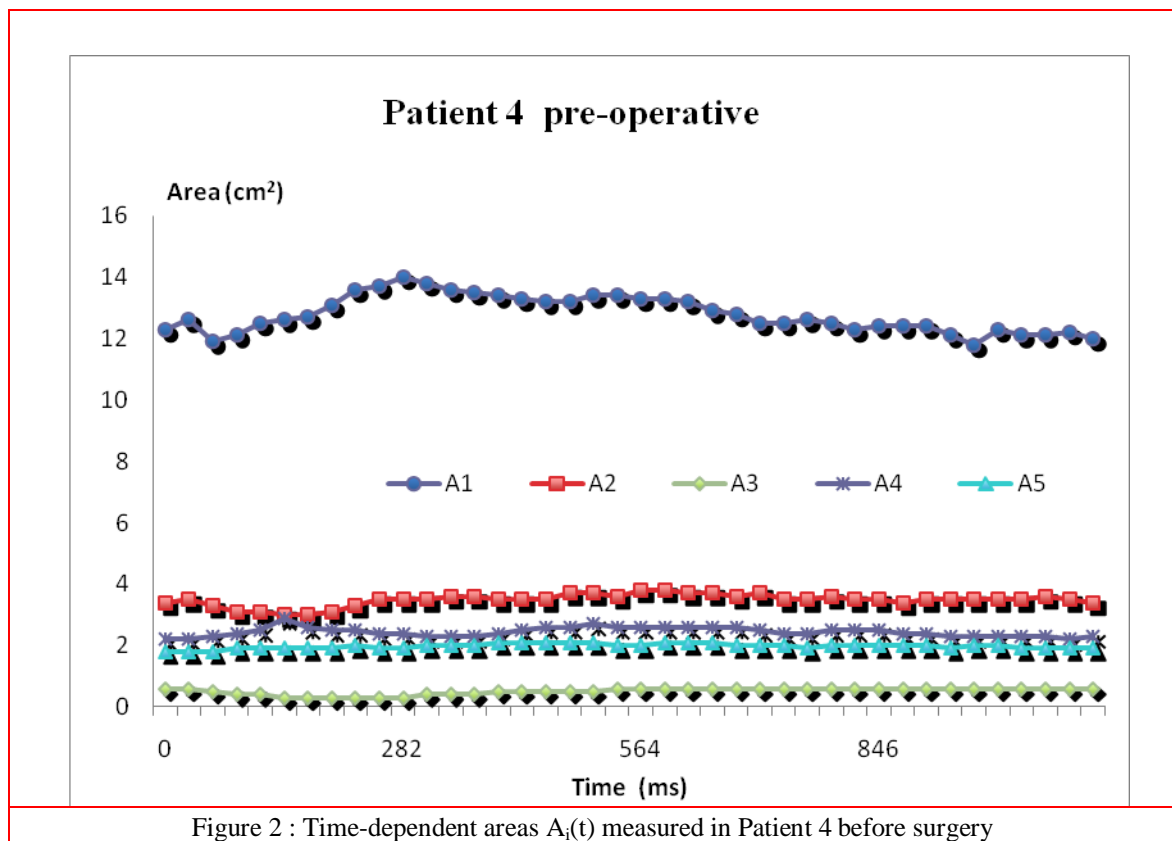

Figure 2 : Time-dependent areas $A_i(t)$ measured in Patient 4 before surgery

Table 2 Preoperative Patient 4 data: mean, minimal and maximal values of the areas $A_i(t)$ (cm^2) and relative maximal dilatation of the aorta in each section S_i, during a cycle.

	S_1	S_2	S_3	S_4	S_5
$A^{mean} \pm SD$	12.8 ± 0.6	3.5 ± 0.2	0.5 ± 0.1	2.4 ± 0.15	2.0 ± 0.1
A^{min}	11.8	3	0.3	2.2	1.8
A^{max}	14	3.8	0.6	2.9	2.1
$(A^{max} - A^{min}) / A^{min}$	0.19	0.27	1	0.32	0.17

Table 3 Areas (in cm^2) of the 5 cross-sections S_i of the aorta: mean value, minimal and maximal values over the cardiac cycle, for every patient after surgery (P_i = Patient "i").

	S_1	S_2	S_3	S_4	S_5
A^{mean}, P_1	11.7 ± 0.5	2.8 ± 0.2	2.9 ± 0.15	2.6 ± 0.4	2.0 ± 0.2
A^{min}, P_1	10.6	2.5	2.7	2.1	1.7
A^{max}, P_1	12.6	3.1	3.2	3.1	2.3
A^{mean}, P_2	6.1 ± 0.3	3.2 ± 0.01	2.9 ± 0.2	3.6 ± 0.3	1.8 ± 0.3
A^{min}, P_2	5.7	3.0	2.6	3.0	1.5
A^{max}, P_2	6.5	3.4	3.2	3.9	2.3
A^{mean}, P_3	8.1 ± 0.6	1.8 ± 0.1	2.6 ± 0.3	2.9 ± 0.1	2.2 ± 0.2
A^{min}, P_3	6.7	1.6	2.1	2.6	2.0
A^{max}, P_3	9.3	1.9	3.1	3.1	2.5
A^{mean}, P_4	11.2 ± 0.9	2.0 ± 0.1	1.4 ± 0.1	2.9 ± 0.4	2.2 ± 0.0
A^{min}, P_4	10.0	1.8	1.2	2.1	2.2
A^{max}, P_4	12.9	2.3	1.5	3.2	2.2

Table 4 Postoperative relative maximal dilatation of the aorta, $(A^{max} - A^{min}) / A^{min}$, in each section S_i, during a cardiac cycle.

	S_1	S_2	S_3	S_4	S_5
Patient 1	0.19	0.24	0.19	0.48	0.35
Patient 2	0.14	0.13	0.23	0.3	0.53
Patient 3	0.39	0.19	0.48	0.19	0.25
Patient 4	0.29	0.28	0.25	0.52	0.0

Table 5 Postoperative indexes of coarctation severities.

	Patient 1	Patient 2	Patient 3	Patient 4
Sev1	1.07	0.86	1.12	0.57

As regards the velocities presented in Figure 4 and Table 7, the striking feature is the elevated velocity at the throat (V_3) secondary to the diameter reduction of the aorta. A rough estimation based on simplified Bernoulli equation ($\Delta P = (\rho V^2)/2$, with a preoperative pressure gradient ΔP of 40 mmHg, would yield a velocity of order 319 cm/s, which is somewhat higher than the values obtained from MRI. However, such a calculation is very approximate and depends also on the precision of the pressure gradient measurement. More convincing is the comparison with the data of Holmqvist *et al.* [16], who made haemodynamic MRI measurements for 13 coarcted patients with different degrees of stenosis. The ranges of velocities they obtain were: 50-130 cm/s above the coarctation, 50-230 cm/s at the level of the coarctation, 30-210 cm/s just below the coarctation, and 30-70 cm/s at the level of the diaphragm.
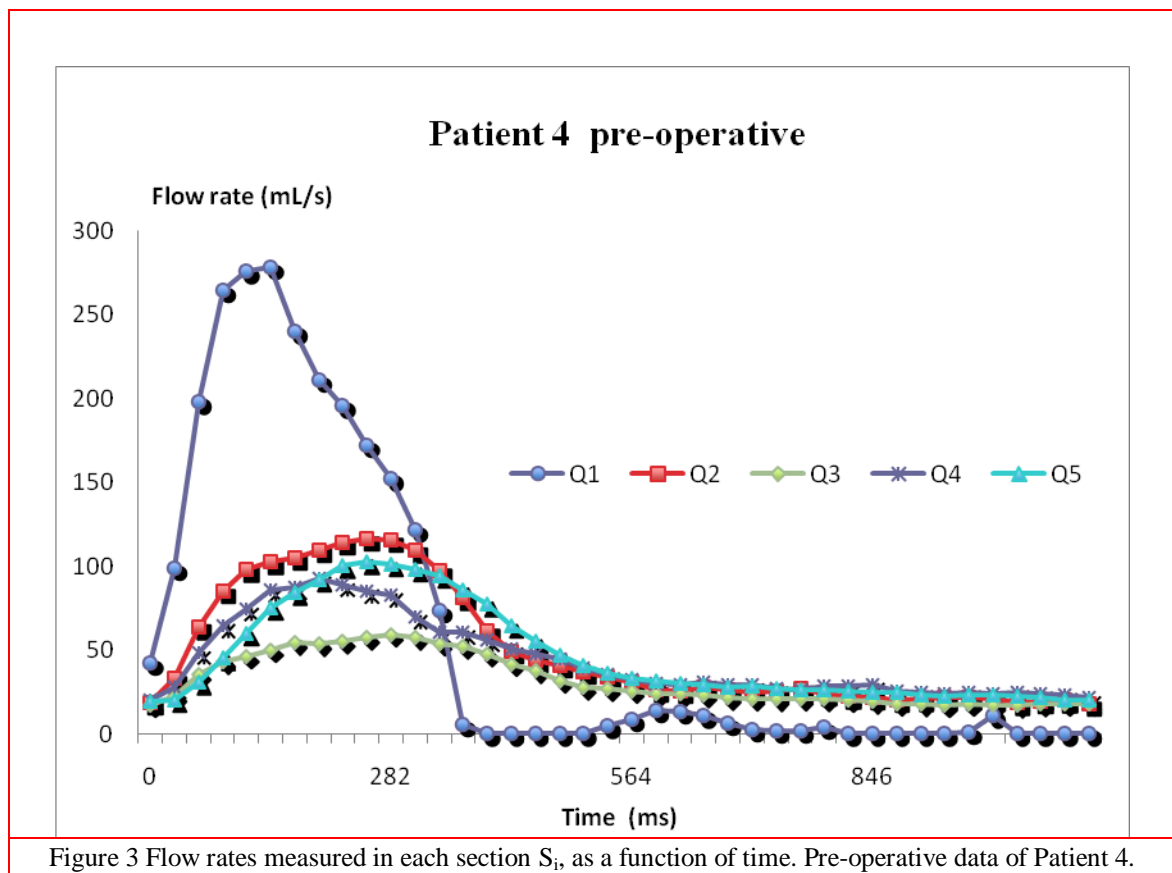

Figure 3 Flow rates measured in each section S_i, as a function of time. Pre-operative data of Patient 4.

Our velocities (Figure 4 and Table 7) fit perfectly well with these data. Goubergrits *et al.* [6] have given slightly higher values: peak systolic flow rates in the ascending aorta from 254 ml/s to 651 ml/s, range of the proportion between the flow in the descending aorta compared to the flow in the ascending aorta from 32.3 % to 75.5 %, and peak systolic Reynolds numbers from 1580 to 10500. However, the patients included in their study present a wide panel of coarctation severities (from 25% to 92% reduction of area).

Reynolds numbers (Table 8) could indicate that some turbulence is present in these aortic flows [3].

Indeed, the narrowing of the aorta causes the formation of two recirculation zones: one is upstream to the stenosis, similar to the other aortic arches, but less pronounced, and the other is immediately downstream to the stenosis. The second one is induced at the outer curvature of the descending aorta by the jet formed by the flow passing through the constriction. Such a jet is typically linked to large flow recirculations and vortices, where kinetic energy of the flow is lost [2]. However, as explained by Stalder et al. [17], the pulse frequency (Womersley number) is also known to play a role in the development of turbulence (because turbulence needs time to develop).

Table 6 Preoperative data of Patient 4. Mean values (over the cardiac cycle) of the flow rates (ml/s) in each section, and the corresponding minimal and maximal values.

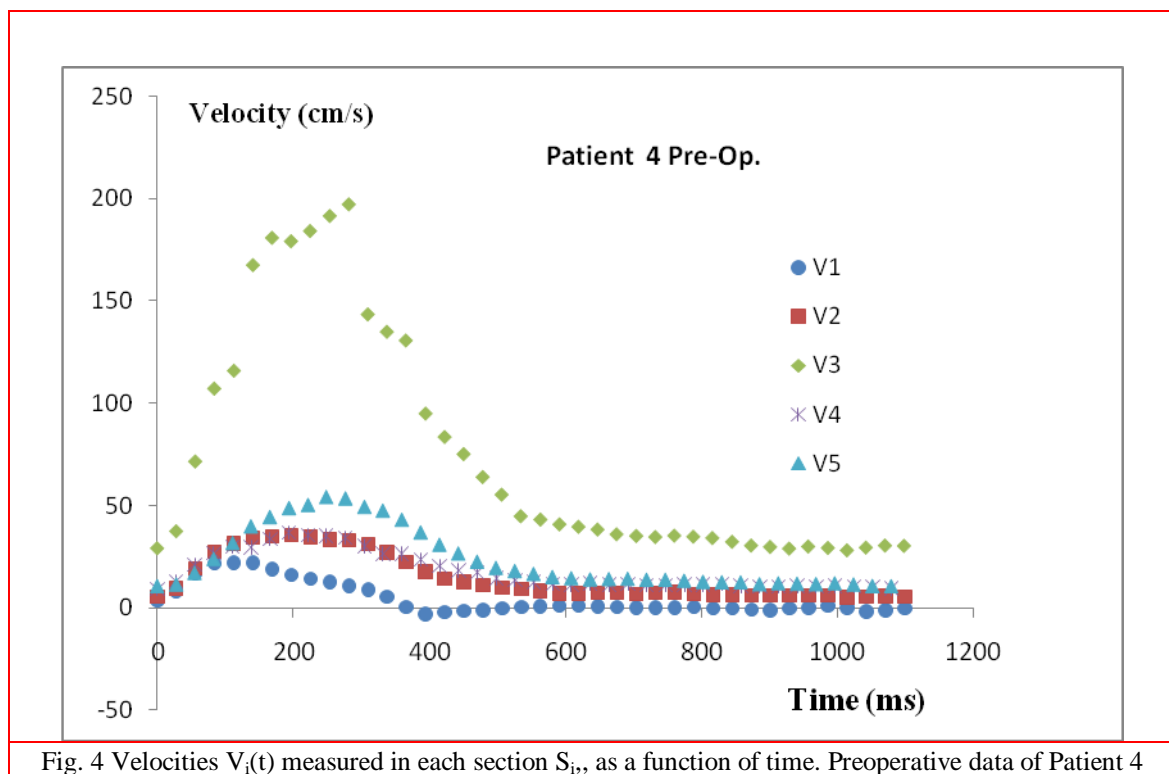|	Q_1	Q_2	Q_3	Q_4	Q_5
$Q^{mean} \pm SD$	89.3 ± 102.4	49.6 ± 35.5	31.8 ± 15	44.1 ± 23.1	46.1 ± 28.7
Q^{min}	-10.0	17.9	16.8	20.4	19.1
Q^{max}	278.5	116.7	59.1	92.4	102.5

Fig. 4 Velocities $V_i(t)$ measured in each section S_i, as a function of time. Preoperative data of Patient 4

Table 7 Preoperative data of Patient 4. Peak systolic velocities (cm/s) in each section S_i.

	V_1	V_2	V_3	V_4	V_5
Vel. max	22.1	35.4	197.0	37.0	53.9

Table 8 Preoperative data of Patient 4. Peak systolic Reynolds number in each section S_i.

	Re_1	Re_2	Re_3	Re_4	Re_5
Re max	2656	2128	3653	1978	2517

Post-operative results for all the Patients (1 to 4)

Postoperative flow rates are presented in the Figures 5 to 8. The corresponding peak systolic flow rates are gathered in Table 9, the mean flow rates in Table 10, the peak systolic velocities in Table 11, and the peak systolic Reynolds numbers in Table 12. Data present some evident dispersion, which is partly due to the variability of patients (Table 1).

The general shape of flow curves is quite similar as preoperative data of Patient 4. Nevertheless, some details can be noticed. For Patient 1, the curves $Q_4(t)$ and $Q_5(t)$ indicated that some collateral flow remains even after surgical repair, which have already been observed by other authors (Figure 3 in [7]). On the contrary, Patient 2 presented harmonious decreasing flows along the aorta, with a regular shift in time. This may be related the surgical technique with a complete reconstruction of the aortic arch. No more collateral flow was detected in this Patient after surgery. The post-operative curve $Q_4(t)$ of Patient 4 has an unexpected shape, that could be due to some technical measurement problem, or to the surgical technique (patch enlargement), or to the angular geometry of the arch. The shape of the aortic arch may also explain some other surprising results for Patients 1 and 3 (curves Q_3 and Q_4).

An increase in flow through the coarctation site after surgical repair was observed for Patient 4, but this increase remained moderate, due to a persistent obstruction after surgical repair (Table 5). The peak systolic values obtained for the velocity and the Reynolds number of Patient 4, in the Section S_4 (Table 11 and 12) are surprisingly low but probably linked to the questionable curve $Q_4(t)$, as explained just above.

Overall, all velocity data (Table 7 for Patient 4 preoperative values and Table 11 for postoperative data) fall exactly in the range computed by Ralovich *et al.* [18] and shown in the Figure 2 of their paper. Before surgery, they obtain velocity values up to 140 cm/s in a moderate narrowing, and after surgery, the range of velocities is reduced (up to 80 cm/s). La Disa *et al.* [19] have also found regions of elevated velocity (up to 100 cm/s) in their computations for CoA patients, which underwent a surgical repair (end-to-end anastomosis).

Fig. 6 Fow rates (ml/s) measured in each section S_i , as a function of time. Postoperative data of Patient 1

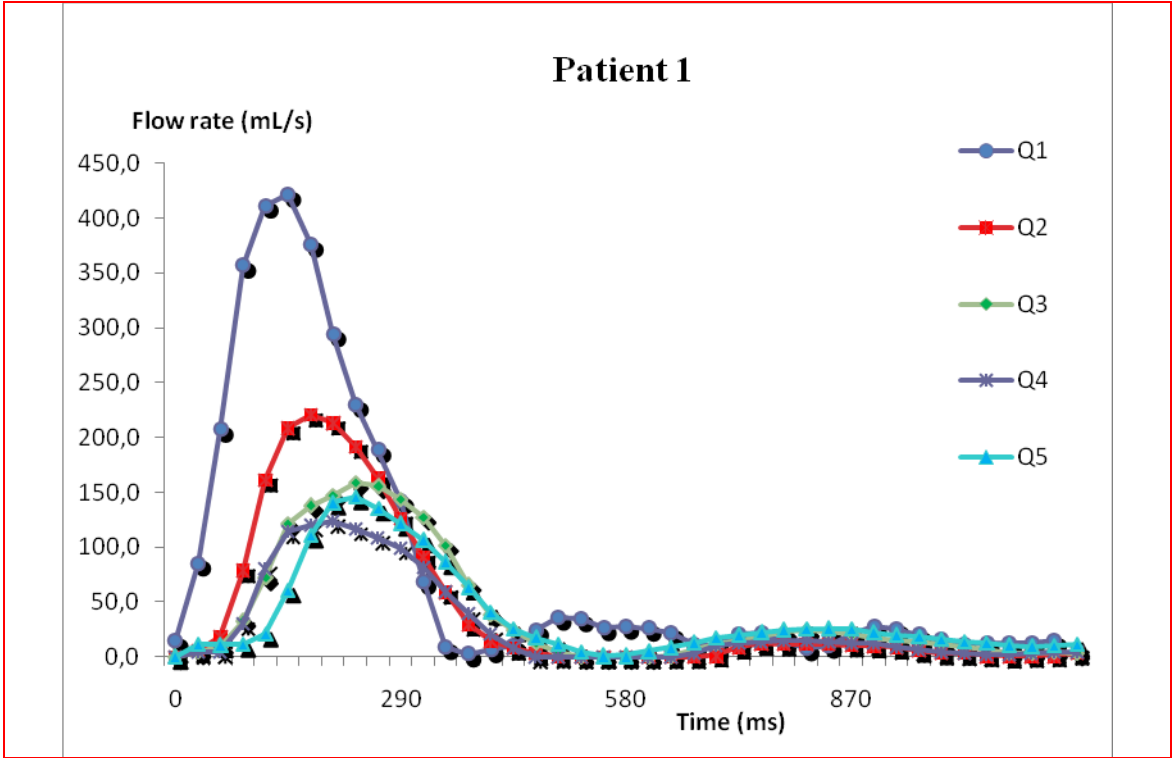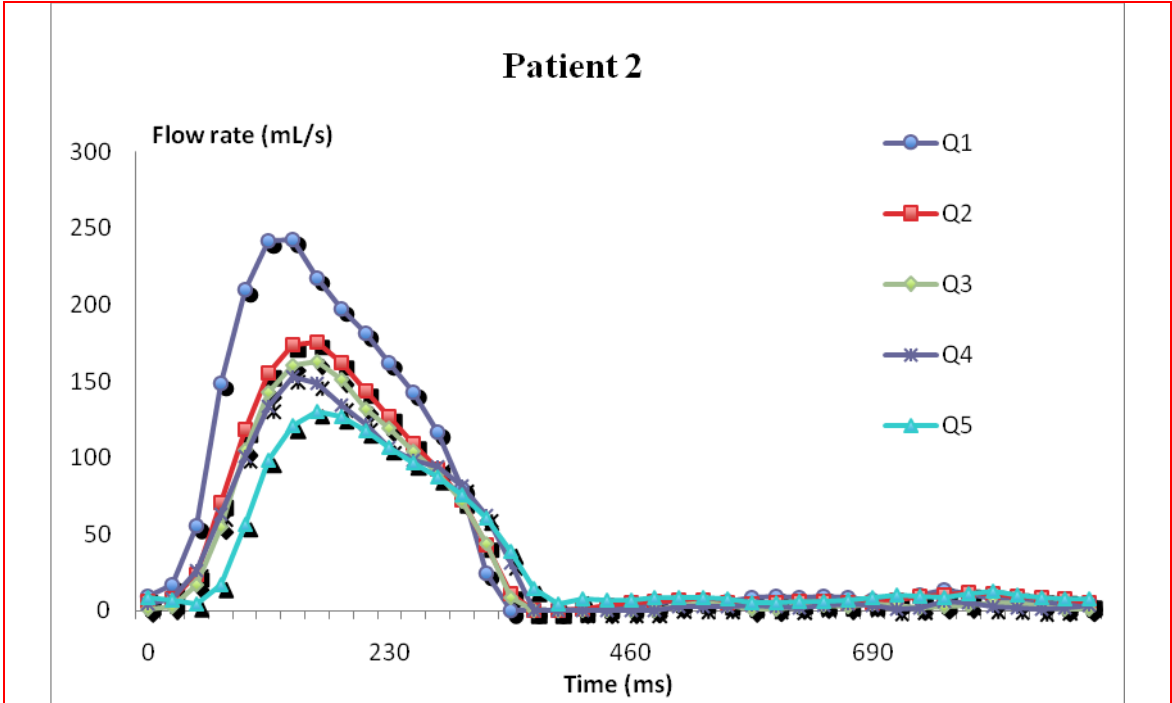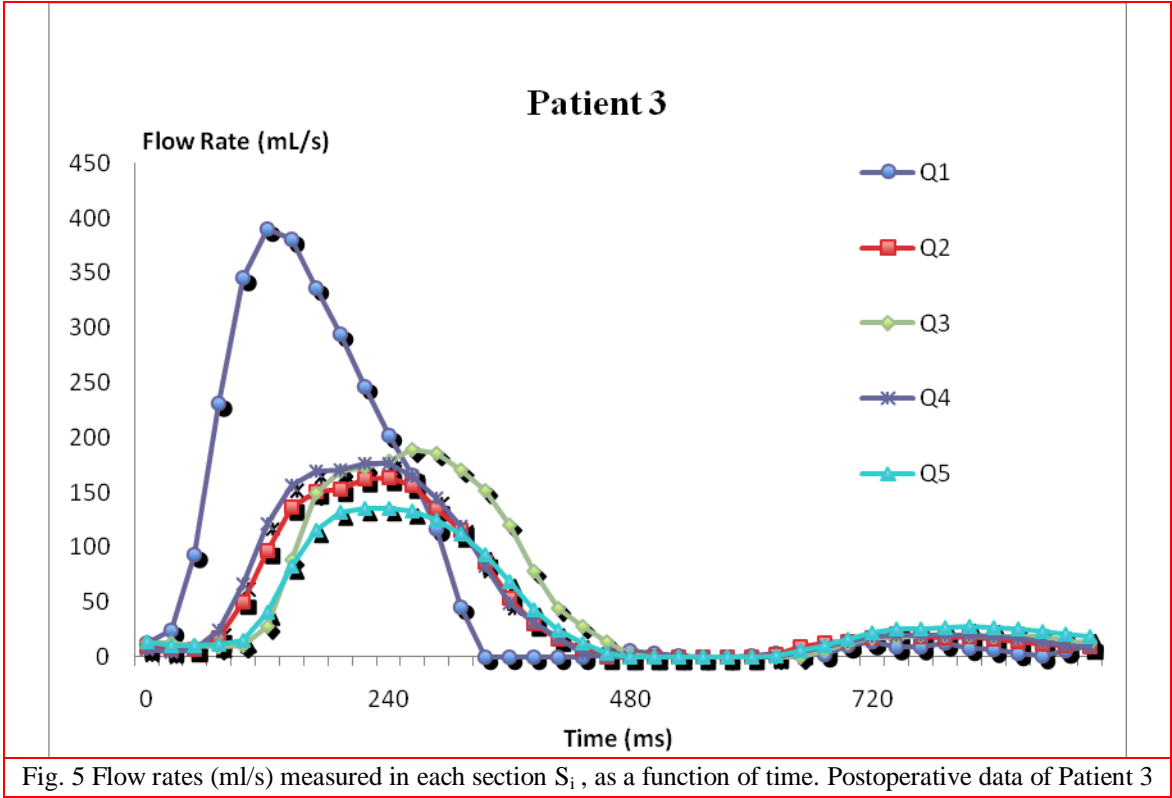Fig. 7 – Flow rates (ml/s) measured in each section S_i, as a function of time. Post-operative data of Patient 2

Fig. 5 Flow rates (ml/s) measured in each section S_i, as a function of time. Postoperative data of Patient 3
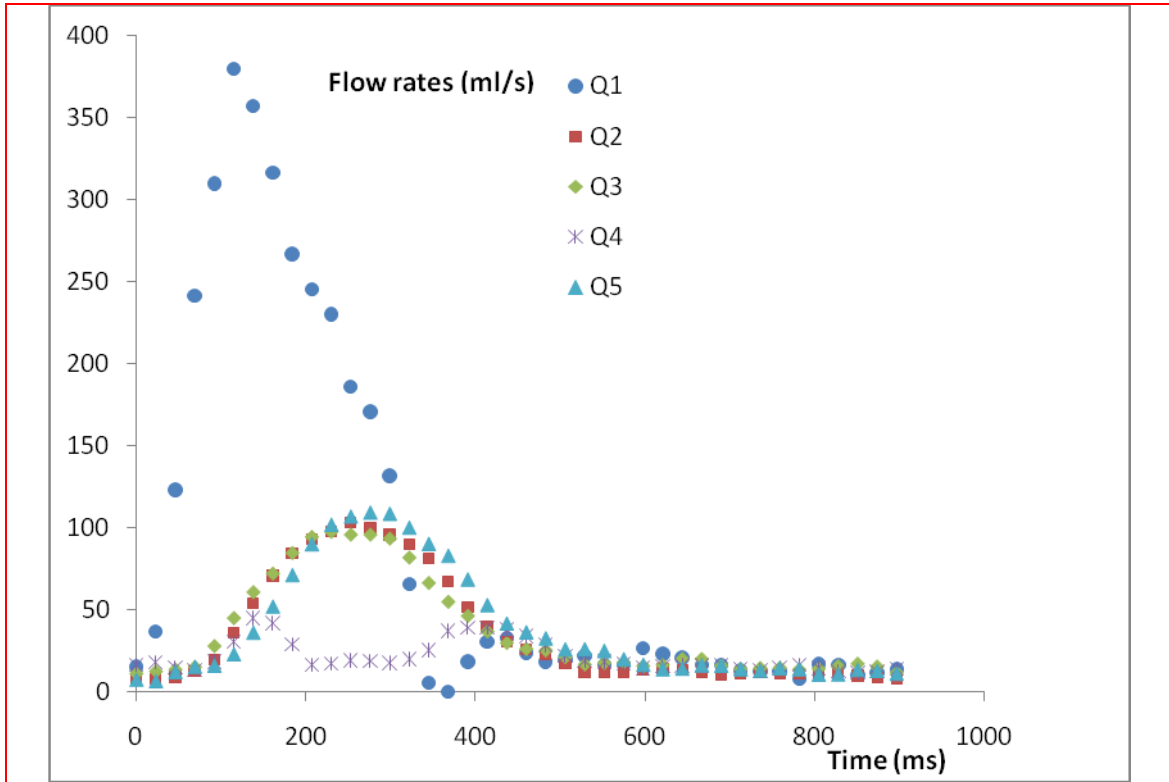
Fig. 8 Flow rates (ml/s) measured in each section S_i, as a function of time. Postoperative data of Patient 4

Table 9   Peak systolic flow rate (ml/s) for Patient 1 to 4, post-op values.

	S_1	S_2	S_3	S_4	S_5
Patient 1	421.1	220.5	158.4	123.3	145.4
Patient 2	242.6	175.7	162.6	152.5	130.3
Patient 3	390.2	163	188.9	176.5	135.6
Patient 4	380	102.9	97.6	44.7	108.9

Table 10   Mean flow rate (ml/s) over the cycle, for Patient 1 to 4, post-op values.

	S_1	S_2	S_3	S_4	S_5
Patient 1	82.1 ± 124.6	49.9 ± 73.5	42.8 ± 52.8	35.1 ± 42.7	36.4 ± 42.2
Patient 2	59.3 ± 82.4	43.0 ± 58.4	40.5 ± 56.9	41.6 ± 53.2	33.7 ± 42.7
Patient 3	90.7 ± 131.5	52.7 ± 58.2	61.0 ± 67.9	58.6 ± 64.7	46.6 ± 46.1
Patient 4	89.6 ± 115.6	35.2 ± 33.4	37.0 ± 30.0	21.3 ± 9.4	38.5 ± 34.1

Table 11   Peak systolic velocities (cm/s) for Patient 1 to 4, post-op values.

	S_1	S_2	S_3	S_4	S_5
Patient 1	35.1	76.0	58.7	50.0	67.0
Patient 2	39.7	58.6	62.5	47.9	67.1
Patient 3	47.0	85.2	72.7	60.9	59.6
Patient 4	33.0	55.5	81.3	15.4	49.5

Table 12   Peak systolic Reynolds for Patient 1 to 4, post-op values.

	S_1	S_2	S_3	S_4	S_5
Patient 1	4098	4383	3263	2640	3318
Patient 2	3315	3434	3414	2855	3048
Patient 3	4585	3974	3966	3508	3027
Patient 4	3793	2527	3016	874	2485

The supra aortic flow rate $Q_{SAV}(t)$

The supra-aortic flow $Q_{SAV}(t)$ represented in Figure 9 are very similar (in shape and amplitude) to other curves of the same type that can be found in the literature , and that present directly the flow rates in the branches leaving the arch (such curves can be found for example in the Figure 1 of the paper of Lantz and Karlsson [20] or in the Figure 10 of the paper of Wittberg et al. [3]).

The difference $Q_1(t) – Q_2(t)$ obviously followed the trends of the curves $Q_1(t)$ and $Q_2(t)$ themselves, according to patients characteristics (Patient 2 had lower blood flows relative to her small morphology). As regards the repartition of the aortic flux between the supra-aortic vessels and the descending aorta, the informations given in the literature differ slightly. Wittberg *et al.* [3] report that about 13% of the flow entering a normal ascending aorta leaves through the brachio-cephalic branch, approximately 5% through the left common carotid and 12% through the left subclavian artery. The remaining 70% flows through the descending aorta. These percentages are slightly modified in case of aortic coarctation (but they do not precise the severity of the constriction in their paper): 17% through the brachio-cephalic branch, 12% through the left common carotid, 9% through the left subclavian artery, and 62% through the descending aorta. Itu *et al.* [21] give a lower proportion of flow into the descending aorta (58.8%), and 25.6 % for the brachio-cephalic artery, 11.3% for the left common carotid artery and 4.3% for the left sub-clavian artery (severity of coarctation not precised). A 75% area reduction in the article of Keshavarz-Motamed *et al.* [22] has showed 30% of total flow going towards supraaortic vessels and 70% going towards the descending aorta. In a previous study [23], the same group of authors has given slightly different informations: for CoA reductions in areas of 50%, 75% and 90%, they have shown that the proportion of inlet aortic flow that enters into the aortic arch arteries is 30%, 40% and 55% respectively (and thus 70%, 60% and 45% goes through the constriction).
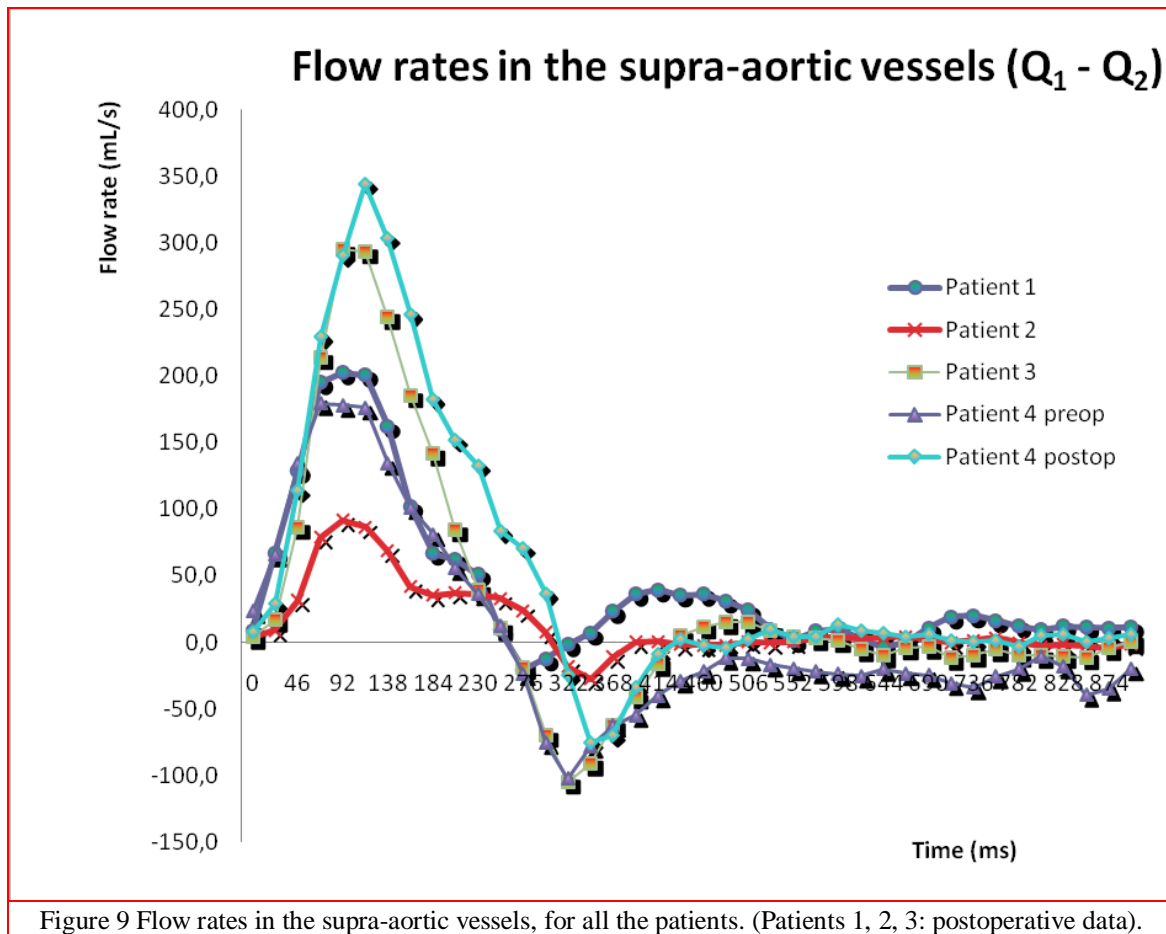
Figure 9 Flow rates in the supra-aortic vessels, for all the patients. (Patients 1, 2, 3: postoperative data).

The collateral flow rate $Q_{col}(t)$

As we have already explained, postoperative flow Q_4 of Patient 4 is not totally reliable. Consequently, the physiological significance of the difference Q_5-Q_4 may be flawed in this case.

In all the other cases, Figure 10 demonstrates the existence of a minimal collateral flow. But this Q_{col} remains lower than 30 ml/s, even for the Patient 4, before surgery. These collateral flows mainly occur during diastole. All patients also have a negative peak in $(Q_5$-$Q_4)$ during systole : Q_4 is thus higher than Q_5 and no collateral flow occurs. This corresponds to the normal situation, when flow in the distal thoracic aorta is less than in the proximal because blood flows away through the intercostal arteries. However, this systolic negative part of the curve is quite reduced for the Patient 4 before surgery, meaning that, most of the time, a collateral flow occurs from the intercostal arteries to the descending aorta.

The persistence of collateral flow after coarctation repair has previously been reported in the literature [7, 24]. Some papers also suggested that the amount of collateral flow as measured by the difference in flow between the distal descending aorta and the proximal descending aorta was

related to the severity of the coarctation [1, 5, 7, 16]. However, some patients with severe coarctation have an inappropriately low volume of collateral flow. Consequently, a wide range of collateral flow data may be found in the literature. We have to note that in patients with coarctation and collateral flow, a temporal shift of the flow curve Q_5 to the diastolic phase of the cardiac cycle may occur. This shift in flow curve could be a result of the increased time required for the blood provided by the collaterals to course through the intercostal arteries into the descending aorta [1], and this is not taken into account when doing the subtraction $Q_5(t)-Q_4(t)$.

Another important point for patients with severe aortic coarctation is that the large amount of collateral blood flow arriving into the descending aorta raises the pressure beyond the coarctation and may minimize the effect of this coarctation on distal aortic pressure. In that case, the pressure gradient is underestimated and may not be a good indicator of the severity of the coarctation. The quantification of the amount of collateral flow might then be more useful [1, 5].
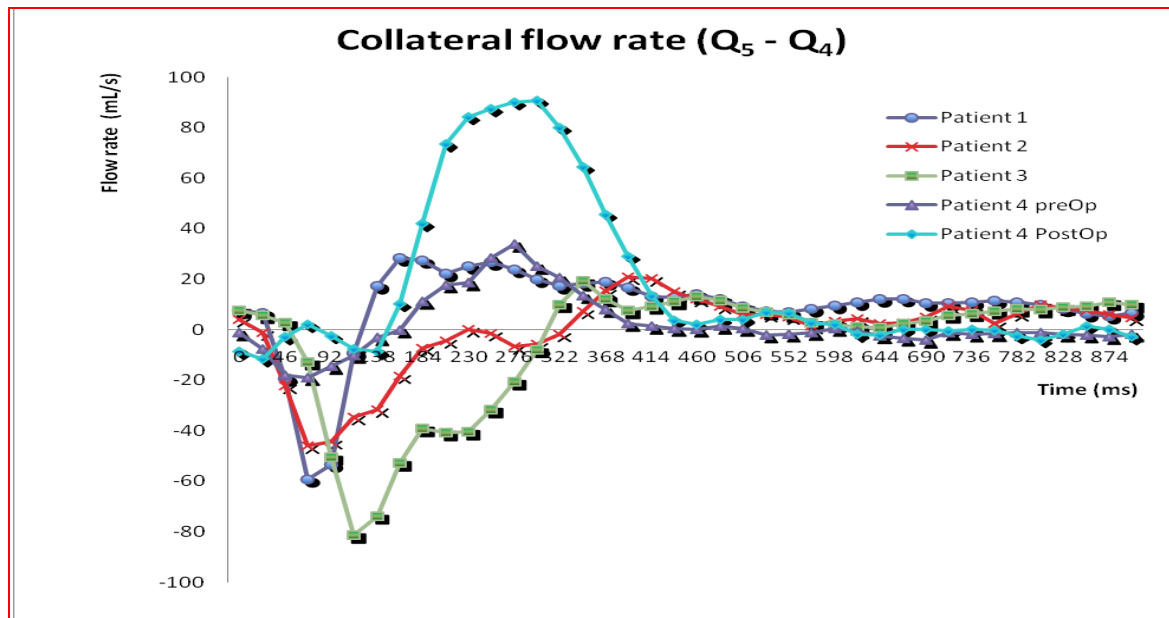
Figure 10   Collateral flow rates, for all the patients

Conclusion

Magnetic Resonance Imaging might be an efficient and accurate tool to evaluate flow changes from the proximal to the distal part of the descending aorta and thereby quantify the volume of collateral flow into the distal descending aorta in patients with a history of aortic coarctation.

Our results are limited by the small number of patients. Yet, our data have shown the importance of monitoring these patients even after corrective surgery. Residual problems such as re-coarctation could be detected earlier by flow perturbations due to some modifications of the arch geometry, modifications of the mechanical properties of the wall of the aortic arch or adjacent

vessels. We hope these elements could help to complete the collateral pathways of some lumped parameter model like the one of Keshavarz-Motamed *et al.* [9].

References

1. Steffens J.C., Bourne M.W., Sakuma H., O'Sullivan M., Higgins C.B. (1994) Quantification of collateral blood flow in coarctation of the aorta by velocity encoded cine magnetic resonance imaging. Circulation 90: 937–43.

2. Hope M., Meadows A., Hope T., Ordovas K., Saloner D., Reddy G., Alley M. and Higgins C. (2010) Clinical evaluation of aortic coarctation with 4D flow MR imaging. Jour. Magn. Res. Imaging, 31: 711-718.

3. Wittberg L. P., van Wyk S., Fuchs L., Gutmark E., Backeljauw P., Gutmark-Little I. (2016) Effects of aortic irregularities on blood flow. Biomech Model Mechanobiol. 15(2): 345–60.

4. LaDisa J.F., Taylor Ch. and Feinstein J. (2010) Aortic coarctation: recent developments in experimental and computational methods to assess treatments for this simple condition. Progress in Pediatric Cardiology 30: 45–49.

5. Muzzarelli S., Meadows A.K., Ordovas K.G., Hope M.D., Higgins C.B., Nielsen J.C., Geva T. and Meadows J.J. (2011) Prediction of hemodynamic severity of coarctation by magnetic resonance imaging. Am J Cardiol. 108: 1335–40.

6. Goubergrits L., Riesenkampff E., Yevtushenko P., Schaller J., Kertzscher U., Hennemuth A., Berger F., Schubert S., Kuehne T. (2015) MRI-based computational fluid dynamics for diagnosis and treatment prediction: clinical validation study in patients with coarctation of aorta. J Magn Reson Imaging, 41: 909–916.

7. Araoz P.A., Reddy G.P., Tarnoff H., Roge C.L., and Higgins Ch.B. (2003) MR findings of collateral circulation are more accurate measures of hemodynamic significance than arm-leg blood pressure gradient after repair of coarctation of the aorta. J Magn Reson Imaging. 17: 177–83.

8. Valverde I., Staicu C., Grotenhuis H., Marzo A., Rhode K., Shi Y., Brown A., Tzifa A., Hussain T., Greil G., Lawford P., Razavi R., Hose R. and Beerbaum P. (2011) Predicting hemodynamics in native and residual coarctation: preliminary results of a rigid wall computational fluid dynamics model (RW-CFD) validated against clinically invasive pressure measures at rest and during pharmacological stress. Jour. CardioVasc. Magn. Res, 13(Supp. 1): 49-52.

9. Keshavarz-Motamed Z., Edelman E.R., Motamed P. K., Garcia J., Dahdah N., and Kadem L. (2015) The role of aortic compliance in determination of coarctation severity: Lumped parameter modeling, in vitro study and clinical evaluation. J Biomech. 48: 4229–37.

10. Kenny D., Polson J., Martin R., Wilson D., Caputo M., Cockcroft J., Paton J., and Wolf A. (2010) Surgical approach for aortic coarctation influences arterial compliance and blood pressure control. Ann. Thor. Surg. 90: 600–604.

11. Ou P., Bonnet D., Auriacombe L., Pedroni E., Balleux F., Sidi D., and Mousseaux E. (2004) Late systemic hypertension and aortic arch geometry after successful repair of coarctation of the aorta. Eur Heart J. 25(20): 1853–9.

12. ESC (European Society of Cardiology) (2014) Guidelines on the diagnosis and treatment of aortic disease. Eur. Heart Jour. 35: 2873–2926.

13. Xu J., Shiota T., Omoto R., Zhou X., Kyo S., Ishii M., Rice M., and Sahn D. (1997) Intravascular ultrasound assessment of regional aortic wall stiffness, distensibility, and compliance in patients with coarctation of the aorta. Am Heart Jour. 134: 93–8.

14. LaDisa J.F., Figueroa C.A., Vignon-Clementel I.E., Kim H. J., Xiao N., Ellwein L.M., Chan F.P., Feinstein J.A., Taylor C.A. and Feinstein J.A. (2011a) Computational simulations for aortic coarctation: representative results from a sampling of patients.   Jour. Biomech. Engin., 133 : 091008-1 to 091008-9.

15. O'Rourke M. and Cartmill T. (1971) Influence of aortic coarctation on pulsatile hemo-dynamics in the proximal aorta. Circulation Vol. XLIV: 281-292.

16. Holmqvist C., Stahlberg F., Hanseus K., Hochbergs P., Sandstrom S., Larsson E.M. and Laurin S. (2002) Collateral flow in coarctation of the aorta with magnetic resonance velocity mapping: correlation to morphological imaging of collateral vessels. Jour. Magn. Res. Imaging. 15: 39-46.

17. Stalder A., Frydrychowicz A., Russe M., Korvink J., Hennig J., Li K., Markl M. (2011) Assessment of flow instabilities in the healthy aorta using flow sensitive MRI. Jour. Magn. Res. Imaging 33: 839-846.

18. Ralovich K., Itu L, Mihalef V, Sharma P, Ionasec R, Vitanovski D, Krawtschuk W., Everett A., Ringel R., Navab N. and Comaniciu D. (2012) Hemodynamic Assessment of Pre- and Post-operative Aortic Coarctation from MRI. In: Ayache et al. (Eds). Medical Image Computing and Computer-Assisted Intervention – MICCAI 2012, Part II, LNCS 7511: 486–93.

19. LaDisa J.F., Dholakia R.J., Figueroa C.A., Vignon-Clementel I.E., Chan F.P., Samyn M.M., Cava J.R., Taylor C.A. and Feinstein J.A. (2011b) Computational simulations demonstrate altered wall shear stress in aortic coarctation patients treated by resection with end-to-end anastomosis. Cong. Heart Dis. 6(5): 432-443.

20. Lantz J. and Karlsson M. (2012) Large eddy simulation of LDL surface concentration in a subject specific human aorta.   Jour. Biomechanics 45: 537-542.

21. Itu L., Sharma P., Passerini T., Kamen A., Suciu C. and Comaniciu D. (2015) A parameter estimation framework for patient-specific hemodynamic computations. Jour. Comp. Physics 281: 316–333.

22. Keshavarz-Motamed Z., Garcia J. and Kadem L. (2013) Fluid dynamics of coarctation of the aorta and effect of bicuspid aortic valve. PLoS ONE 8(8) : e72394.

23. Keshavarz-Motamed Z., Garcia J., Maftoon N., Bedard E., Chetaille P. and Kadem L. (2012) A new approach for the evaluation of the severity of coarctation of the aorta using Doppler velocity index and effective orifice area: in vitro validation and clinical implications. Jour. Biomechanics 45: 1239–1245.

24. Ross J.K., Monro J.L. and Sbokos C.G. (1975) Late complications of surgery for coarctation of the aorta. Thorax 30: 31–39.